RIBOSOMAL CRYSTALLOGRAPHY: PEPTIDE BOND FORMATION, CHAPERONE ASSISTANCE, AND ANTIBIOTICS INACTIVATION

ADA YONATH
Department of Structural Biology
Weizmann Institute, Rehovot 76100, Israel
Tel: 972-8-9343028
Fax: 972-8-9344154
E-mail: ada.yonath@weizmann.ac.il

Abstract: The peptidyl transferase center (PTC) is an arched void has dimensions suitable for accommodating the 3′ ends of the A-and the P-site tRNAs. It is situated within a universal sizable symmetrical region that connects all ribosomal functional centers involved in amino-acid polymerization. The linkage between the elaborate PTC architecture and the A-site tRNA position revealed that the A- to P-site passage of the tRNA 3′ end is performed by a rotatory motion, which is synchronized with the overall tRNA/mRNA sideways movement, and leads to stereochemistry suitable for peptide bond formation and for substrate mediated catalysis, thus suggesting that the PTC evolved by gene fusion. Adjacent to the PTC is the entrance of the protein exit tunnel, shown to play active roles in sequence-specific gating of nascent chains and in responding to cellular signals. This tunnel also provides a site that may be exploited for local cotranslational folding and seems to assist nascent chain trafficking into the hydrophobic space formed by the first bacterial chaperone, the trigger factor. Many antibiotics target ribosomes. Although the ribosome is highly conserved, subtle sequence and/or conformational variations enable drug selectivity, thus facilitating clinical usage. Comparisons of high-resolution structures of complexes of antibiotics bound to ribosomes from eubacteria resembling pathogens, to an archaeon that shares properties with eukaryotes and to its mutant that allows antibiotics binding, demonstrated the unambiguous difference between mere binding and therapeutical effectiveness. The observed variability in antibiotics inhibitory modes, accompanied by the elucidation of the structural basis to antibiotics mechanism justifies expectations for structural based improved properties of existing compounds as well as for the development of novel drugs.

Keywords: antibiotics selectivity; elongation arrest; resistance; ribosomal antibiotics; ribosomal symmetrical region; trigger factor.

1. Introduction

Ribosomes are giant ribonucleoprotein cellular assemblies that translate the genetic code into proteins. They are built of two subunits of unequal size that associate upon the initiation of protein biosynthesis to form a functional particle and dissociate once this process is terminated. The bacterial ribosomal subunits are of molecular weights of 0.85 and 1.45 MDa. The small

J. D. Puglisi (ed.), Structure and Biophysics – New Technologies for Current Challenges in Biology and Beyond, 127–153.

subunit (called 30S in prokaryotes) contains an RNA chain (called 16S) of about 1,500 nucleotides and 20−21 proteins, and the large one (called 50S in prokaryotes) has two RNA chains (23S and 5S RNA) of about 3,000 nucleotides in total, and 31−35 proteins. Protein biosynthesis is performed cooperatively by the two ribosomal subunits and several nonribosomal factors, assisting the fast and smooth processivity of protein formation, required for cell vitality. While elongation proceeds, the small subunit provides the decoding-center and controls translation fidelity, and the large one contains the catalytic site, called the peptidyl-transferase-center (PTC), as well as the protein exit tunnel.

mRNA carries the genetic code to the ribosome, and tRNA molecules bring the protein building block, the amino acids, to the ribosome. These L-shape molecules are built mainly of double helixes, but their two functional sites, namely the anticodon loop and the CCA 3′end, are single strands. The ribosome possesses three tRNA binding site, the A-(aminoacyl), the P-(peptidyl), and the E-(exit) sites. The tRNA anticodon loop interacts with the mRNA on the small subunit, whereas the tRNA acceptor stem, together with the aminoacylated or peptidylated tRNA 3′ends interacts with the large subunit. Hence, the tRNA molecules are the entities combining the two subunits, in addition to the intersubunit bridges, which are built of flexible components of both subunits. The elongation cycle involves decoding, the creation of a peptide bond, the detachment of the P-site tRNA from the growing polypeptide chain and the release of a deacylated tRNA molecule and the advancement of the mRNA together with the tRNA molecules from the A- to the P- and then to the E-site. This motion is driven by GTPase activity.

Two decades of experimentation (reviewed in Yonath, 2002) yielded high resolution structures of the small ribosomal subunit from *Thermus thermophilus*, T30S (Schluenzen et al., 2000; Wimberly et al., 2000), of the large subunit from the archaeon *Haloarcula marismortui*, H50S (Ban et al., 2000), from the eubacterium *Deinococcus radiodurans*, D50S (Harms et al., 2001) and recently also of the entire apo 70S ribosome (Schuwirth et al., 2005). Together with the additional structures of their complexes with substrate analogs (Bashan et al., 2003a; Hansen et al., 2002a; Nissen et al., 2000; Schmeing et al., 2002; Yusupov et al., 2001) and with a medium resolution structure of the whole ribosome from *T. thermophilus*, T70S in complex with three tRNA molecules (Yusupov et al., 2001), these structures shed light on the vast amount of biochemical knowledge accumulated in over five decades of ribosomal research.

The actual reaction of peptide bond formation is performed by a nucleophilic attack of the primary amine of the A-site amino acid on the carbonyl carbon of the peptidyl tRNA at the P-site. This reaction can be performed by tRNA 3′end analogs. Puromycin is a universal inhibitor mimicking the tip of the tRNA 3′end. Its binding to the ribosome in the presence of an active donor substrate can result in peptide bond formation uncoupled from the translocation of the A-site tRNA, namely from the polymerization of the amino acids into polypeptides. Puromycin has been commonly used as a minimal substrate for investigating the formation of peptide bonds, in a process called the “fragment reaction”, which yields a single peptide bond.

The finding that ribosomal RNA catalyzes the “fragment reaction” (Noller et al., 1992); the localization of the PTC in an environment rich in conserved nucleotides (Harms et al., 2001; Yusupov et al., 2001) the usage of puromycin derivatives bound to the partially disordered large

subunits, H50S (Nissen et al., 2000), together with a compound originally presumed to resemble the reaction intermediate (Moore and Steitz, 2003), but later found to be wrongly assigned (Schmeing et al., 2005a) led to the suggestion that ribosome catalysis resembled the reverse reaction of serine proteases, and that specific ribosome nucleotides participate in the chemical events of peptide bond formation, as a "general base" (Nissen et al., 2000).

Biochemical, kinetic, and mutational results (Barta et al., 2001; Polacek et al., 2003; Sievers et al., 2004; Thompson et al., 2001; Weinger et al., 2004; Youngman et al., 2004) and the finding that the PTC conformation in crystalline H50S hardly resembles the active one (Bayfield et al., 2001), challenged this hypothesis, and indicated that there is no ground for the expectation that a complex assembly such as the ribosome catalyzes protein biosynthesis by the reverse of a common enzymatic mechanism. Indeed, the well-ordered structure of the large ribosomal subunit from *D. radiodurans*, D50S (Harms et al., 2001), determined under conditions resembling its optimal growth environment, raveled that the striking ribosomal architecture provides all structural elements enabling its function as a amino acid polymerase that ensures proper and efficient elongation of nascent protein chains in addition to the formation of the peptide bonds (Agmon et al., 2003, 2004, 2005; Baram and Yonath, 2005; Bashan and Yonath, 2005; Bashan et al., 2003a, b; Yonath, 2003a, b; 2005; Zarivach et al., 2004).

Being a prominent key player in a vital process, the ribosome is targeted by many antibiotics of diverse nature. Consequently, since the beginning of therapeutic administration of antibiotics, ribosomal drugs have been the subject to numerous biochemical and genetic studies (reviewed in Auerbach et al., 2002, 2004; Courvalin et al., 1985; Gale et al., 1981; Gaynor and Mankin, 2003; Katz and Ashley, 2005; Knowles et al., 2002; Poehlsgaard and Douthwaite, 2003; Sigmund et al., 1984; Spahn and Prescott, 1996; Vazquez, 1979; Weisblum, 1995; Yonath, 2005; Yonath and Bashan, 2004). These findings were enforced by the lessons learned from the high resolution structures of their complexes with ribosomal particles (Berisio et al., 2003a, b; Brodersen et al., 2000; Carter et al., 2000; Hansen et al., 2002b, 2003; Harms et al., 2004; Pfister et al., 2004, 2005; Pioletti et al., 2001; Schluenzen et al., 2001, 2003, 2004; Tu et al., 2005), which were found indispensable for illustrating the basic mechanisms of antibiotics activity and synergism. They also provided the structural basis for mechanisms of antibiotic resistance and enlightens the principles of antibiotics selectivity, namely the discrimination between pathogens and eukaryotes, the key for therapeutical usefulness (Auerbach et al., 2004; Yonath, 2005; Yonath and Bashan, 2004).

Since X-ray crystallography requires diffracting crystals, and since so far no ribosomes from pathogenic bacteria could be crystallized, the crystallographic studies are confined to the currently available crystals. The findings that *E. coli* and *T. Thermophilus* are practically interchangeable (Gregory et al., 2005; Thompson and Dahlberg, 2004) and that both crystallizable ribosomes are from eubacteria which resemble pathogens, permit considering them as suitable pathogen models for ribosomal antibiotics. Genetically engineered pathogen models, such as *Mycobacterium smegmatis*, can also serve as pathogen models. These should be advantageous, as they can provide isogenic mutations (Pfister et al., 2004). Similarly, for mutagenesis studies species with single rRNA operon chromosomal copy, such as *Halobacterium halobium* (Mankin and Garrett, 1991; Tan et al., 1996) are beneficial. Additional concern

relates to the relevance of the crystallographic results. The ability to rationalize biochemical, functional and genetics observations by the crystallographic structures demonstrate the inherent reliability of the crystallographic results. The consistencies of drug locations with biochemical and resistance data, alongside the usage of crystalline complexes obtained at clinically relevant drug concentrations, manifest further the reliability of the crystallographic results. Last, the similarities of the structures of T30S wild type as well as of its complexes with antibiotics, elucidated by two independent laboratories (Brodersen et al., 2000; Carter et al., 2000; Pioletti et al., 2001; Schluenzen et al., 2000; Wimberly et al., 2000), indicate that dissimilarities observed crystallographically reflect genuine variability in drug binding modes.

This article focuses on the ribosomal architectural elements that govern both the positional and the chemical contributions to the catalysis of peptide bond formation, sheds light on the essentiality of accurate substrate placement and portrays the parameters dictating it; points at evolution aspects implicated by the ribosomal symmetry; describes how the first chaperon to be encountered by the nascent chain contributes to the mature protein correct folding; and also points at a possible correlation between peptide bond formation, nascent protein progression, cotranslational folding, and cellular regulation. It also relates the structural findings associated with ribosomal antibiotics action and highlights the unique achievements of these studies as well as their shortcoming. Full coverage of the vast amount of biochemical, structural, and medical knowledge is beyond the scope of this article. Instead, it emphasizes the structural finding associated with antibiotics selectivity and synergism, and describes current issues concerning to the acute problem of resistance to antibiotics.

2. Peptide Bond Formation

2.1. SYMMETRY WITHIN THE ASYMMETRIC RIBOSOME

The recently determined three-dimensional structures of ribosomal particles from eubacteria and archaea revealed that the interface surfaces of both subunits are rich in RNA (Figure 1), and localized the PTC in a protein-free environment the middle of the large subunit, thus confirming that the ribosome is a ribozyme. Further analysis, showed that the peptide bond is being formed within a universal sizable symmetrical region (Figure 2), containing ~180 nucleotides (Agmon et al., 2003, 2004, 2005; Baram and Yonath, 2005; Bashan and Yonath, 2005; Bashan et al., 2003a, b; Yonath, 2003a, b, 2005; Zarivach et al., 2004). The symmetrical region is located in and around the PTC, and its symmetrical axis, which is directed into the protein exit tunnel, passes through the peptidyl transferase center, midway between the RNA features shown to host the 3′ends of the A- and the P- sites tRNA.

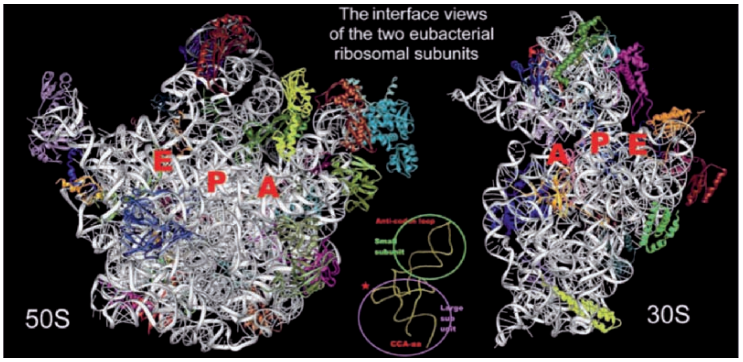

Figure 1. The two ribosomal subunits. The small (30S) and the large (50S) ribosomal subunit, from *T. thermophilus* (Schluenzen et al., 2000) and *D. radiodurans* (Harms et al., 2001), respectively, showing their intersubunit interfaces. In both, the ribosomal RNA is shown as *silver ribbons*, and the ribosomal proteins main chains in different colors. A, P, E designate the approximate locations of the A-,P-, and E- tRNA anticodons on the small subunit, and the tRNA beginning of the tRNA acceptor stems (*the red star on the inserted figure*) on the large one. The regions of tRNA interactions with each subunit are shown on the tRNA molecule, *inserted in the middle*. The *red star* indicates the position at which the tRNA acceptor stem meets the large subunit.

Although first identified in D50S, this symmetrical region seems to be a universal ribosomal feature, as it is present in all known structures of the large ribosomal subunit (Figure 2). The symmetrical region extends far beyond the vicinity of the peptide synthesis location and interacts, directly or through its extensions, with all ribosomal functional features that are relevant to the elongation process: the tRNA entrance and exit regions, namely the L7/L12 stalk and the L1 arm, respectively, the peptidyl transferase center, and the bridges connecting the two subunits (Figure 2), among which bridge B2a resides on the PTC cavity and reaches the vicinity of the decoding center in the small subunit (Yusupov et al., 2001). The 3′ends of the A- and the P- tRNAs bind to the PTC, and even the 3′ end of the E-site tRNA contacts the neighborhood of the symmetry region edge in the T70S complex (Yusupov et al., 2001) but not in H50S complexed with a fragment of the E-site tRNA (Schmeing et al., 2003). Hence, the spatial organization of this region and its central location may enable signal transmission between the remote locations on the ribosome (Agmon et al., 2003).

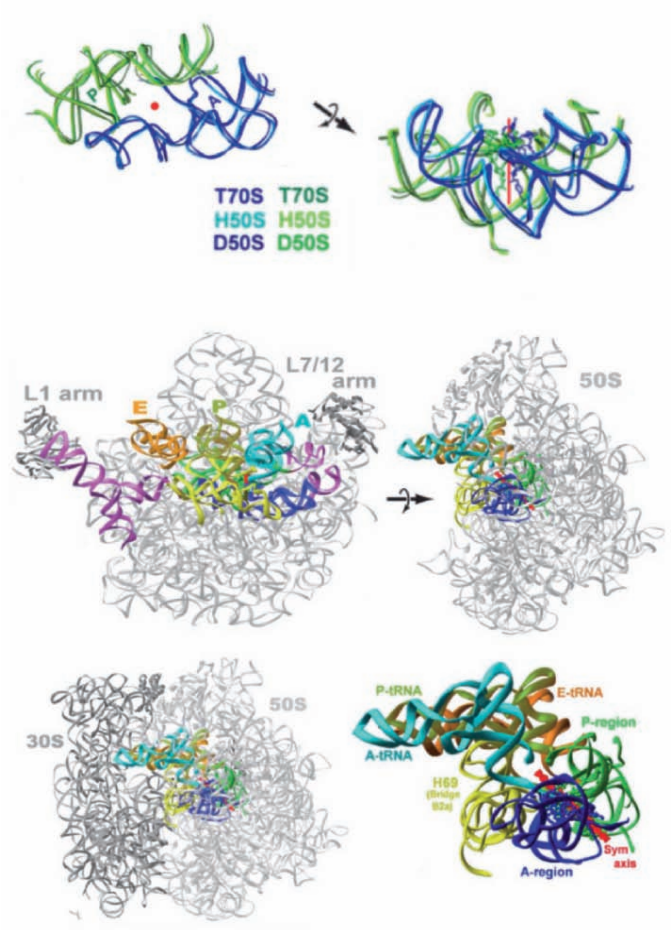

Figure 2. The symmetrical region within the large ribosomal subunit.Throughout, the part containing the A-loop (namely the site of A-site tRNA 3′end) is *blue* (called: *A-region*), and the corresponding one, containing the P-site tRNA 3′end, is *green*. Similarly, the A-site tRNA mimic is shown in *blue* and the derived P site tRNA is *green*. The symmetry axis is shown in *red*. (a) Two orthogonal views (*top* and *side, respectively*) of the superposition of the backbone of the symmetrical regions in all known structures: the entire ribosome from T70S (PDB 1GIY), D50S (PDB 1NKW), and H50S (PDB 1JJ2). Note that the A-site mimic and the derived P-site are incorporated into the side view. *Middle and bottom*: The symmetry related region within the large subunit (*upper panel*) and the entire ribosome (*bottom left*). The direct extensions of the symmetrical region are shown in *purple*. Ribosomal RNA in shown is *gray*

2.2. THE RIBOSOME IS A POLYMERASE

Located at the bottom of a V-shaped cavity (Figure 3), the PTC is an arched void with dimensions suitable for accommodating the 3′ends of the A- and the P-site tRNAs. Each of the symmetry related subregions contains half of the PTC, namely either the A- or the P-site, and the axis relating them by ~180° rotation, is located in the middle of the PTC, midway between the two tRNA binding sites. In a complex of D50S with a 35-nucleotides oligomers mimicking the aminoacylated-tRNA acceptor stem, called ASM (Figure 3), the bond connecting the 3′end with the acceptor stem was found to roughly coincide with the symmetry axis (Bashan et al., 2003a), suggesting that tRNA A → P-site passage is a combination of two independent, albeit synchronized motions: a sideways shift of most of the tRNA molecules, performed as a part of the overall mRNA/tRNA translocation, and a rotatory motion of the tRNA 3′end within the PTC. The path provided by the rotatory motion is confined by the PTC rear wall and by two nucleotides that bulge from the front wall into the PTC center.

Simulation of the rotatory motion (Figure 3) revealed that it is navigated and guided by striking architectural design of the PTC, and that it terminates in a stereochemistry appropriate for a nucleophilic attack of the A-site amino acid on the carbonyl carbon of the peptidyl tRNA at the P-site (Agmon et al., 2003, 2005; Bashan et al., 2003a, b). The spatial match between the PTC rear wall and the contour of the tRNA aa-3′end, formed by the rotatory motion, indicates that it provides the template for the translocation path. From the other side of the PTC, two universally conserved nucleotides A2602 and U2585 (*E. coli* nomenclature, throughout), bulge towards the PTC center (Figures 3) and seem to anchor and/or propel the rotatory motion (Agmon et al., 2003, 2004, 2005; Baram and Yonath, 2005; Bashan et al., 2003a, b; Polacek et al., 2003; Zarivach et al., 2004).

Importantly, the derived P-site tRNA 3′end forms all interactions found biochemically (e.g. Bocchetta et al., 1998; Green et al., 1997) and the orientation of the so created peptide bond is adequate for the ribosomal subsequent tasks, including the release of the peptidyl-tRNA and the entrance of the nascent protein into the exit tunnel. Hence, it appears that the ribosome provides a striking architectural frame, ideal for amino acid polymerization. Thus, the ribosome functions as an enzyme, a ribozyme, responsible not only to peptide bond formation, but also for the successive reactions, namely the creation of polypeptides that can eventually acquire their functional fold (Agmon et al., 2003, 2004, 2005; Bashan et al., 2003a; Zarivach et al., 2004).

ribbons. The positions of the docked three tRNA molecules, as seen in the complex of T70S (PDB 1GIY) are also shown, to indicate their relationship to the symmetry related area. The *gold* feature is the intersubunit bridge (B2a) that combines the two ribosomal active sites. An enlarged view of the symmetry-related region is shown in *right bottom corner*. Note the strategic location of H69, which bridges the two subunits, and plays a major role in A-site tRNA accurate placement.

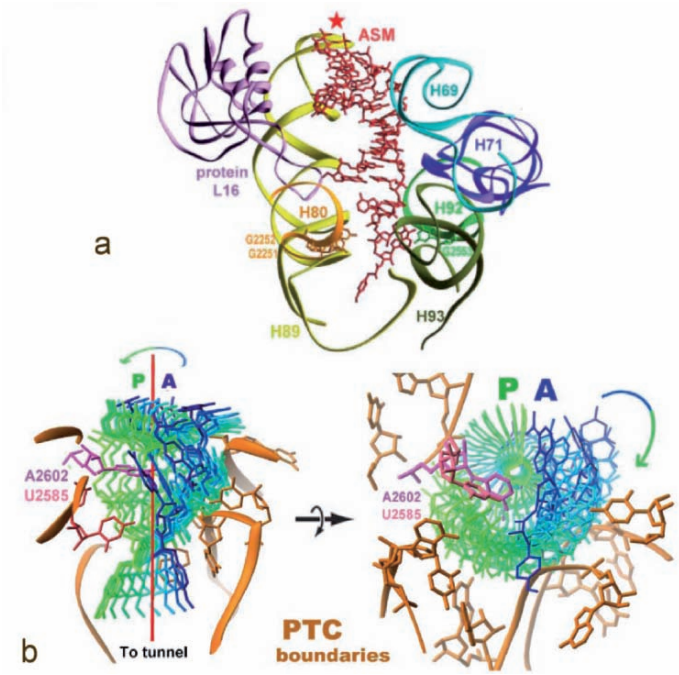

Figure 3. The rotatory motion. Throughout, the part containing the A-loop (namely the site of A-site tRNA 3′end) is *blue* (called: *A-region*), and the corresponding one, containing the P-site tRNA 3′end, is *green*. Similarly, the A-site tRNA mimic is shown in *blue* and the derived P-site tRNA is *green*. The symmetry axis is shown in *red*. (a) The PTC pocket, including ASM, an A-site substrate analog, which is represented by atoms in *red*. The *red star* indicates the position at which the tRNA acceptor stem meets the large subunit, as in Figure 1. The RNA components of the PTC pocket are numbered according to *E. coli* nomenclature (also shown in Figure 5) and colored differently. Note the remote interactions positioning the substrate, as well as the universal contributors to the 3′end base pairs (*a single basepair at the A-site, and two in the P-site*). (b) Two orthogonal snapshots (*sideways and from the tunnel into the PTC*) of intermediate stages (*represented by gradual transformation from blue to green*) in the motion of the A-site tRNA CCA from the A- to the P-site. The two front-wall bulged nucleotides are shown in *pink* and *magenta*. The simulation was performed by rotating the ASM aminoacylated 3′end by (10 times 18° each) within D50S PTC, around the bond connecting the ASM 3′end with its acceptor stem, accompanied by a 2 Å shift in the direction of the tunnel, as implied by the overall spiral nature of the PTC template. The *blue-green round arrows* show the rotation direction. The ribosomal components belonging to the PTC rear wall, that confine the exact path of the rotatory motion, are shown in *gold*. The two front wall flexible nucleotides, A2602 and U2585, are colored in *magenta* and *pink*, respectively.

2.3. SUBSTRATE POSITIONING AND PTC TOLERANCE

Positioning reactants in orientation suitable for chemical reactions is performed by almost all biocatalysts (Jencks, 1969, reissued 1987). Different from enzymes catalyzing a single chemical reactions, such as proteases, and similar to other polymerases, the ribosome provides the

means not only for the chemical reaction (peptide bond formation), but also for substrates motions required for the processivity of peptide bond formation, namely for amino acid polymerization. However, a prerequisite for achieving the ribosome contribution is accurate substrate placement (Yonath, 2003a, b).

The universal Watson–Crick base pair between C75 of A- site tRNA terminus and G2553 (Figure 3) (Kim and Green, 1999), and its symmetrical mate at the P-site, namely the base pair between C75 and G2251, exist in all known structures (Bashan et al., 2003a; Hansen et al., 2002a; Nissen et al., 2000; Schmeing et al., 2002; Yusupov et al., 2001). Positioning governed solely by this base pair is sufficient for entropy driven peptide -bond formation (Gregory and Dahlberg, 2004; Sievers et al., 2004). However, it may not suffice for allowing smooth amino acid polymerization, as shown by the correlation found between the rates of peptide bond formation and the substrate type. Thus, compared to the reaction rate with full size tRNAs, when using the minimal substrate puromycin, such as the "fragment reaction" reactants, the peptide bond is being formed at significantly reduced rates (Moore and Steitz, 2003). Consistently, the locations and orientations of all "fragment reaction" reactants in ribosomal crystals indicate a need to undergo repositioning and/or rearrangements in order to participate in peptide bond formation (Moore and Steitz, 2003; Yonath, 2003b). This time-consuming process can be responsible to the slowness of the "fragment reaction". These observations indicate that the A-site base pairing is not sufficient for accurate tRNA placement, essential for performing the rotatory motion. As the main structural difference between fragment reaction reactants and full-size tRNA is the substrates relative sizes, it appears that accurate positioning is achieved by remote interactions of the A-site tRNA acceptor stem with the upper part of the PTC cavity (Agmon et al., 2003; Yonath, 2003a, b).

Remote interactions cannot be formed by substrate analogs that are too short to reach the PTC cavity upper part, as "fragment reaction" participants, or when helix H69, the remote interactions mate at the PTC upper end (Figures 2 and 3) is disordered, as in H50S structure (Ban et al., 2000; Nissen et al., 2000). It appears, therefore, that the CCA base pairing contributes to the overall positioning of the 3′end of the aminoacylated tRNA, whereas the efficiency of peptide bond formation depends on the tRNA remote interactions. The rotatory motion guides the A-site tRNA to land at the P-site in an orientation appropriate for the creation of the two basepairs. This double basepair seem to stabilize the orientation of P-site tRNA at the conformation essential for the P-site tRNA catalytic role in peptide bond formation (Dorner et al., 2002; Weinger et al., 2004). Hence, the rotatory motion not only leads to a configuration suitable for peptide bond formation (Agmon et al., 2003; Bashan et al., 2003a), it also places the reactants at a distance reachable by the O2' of the P- site tRNA A76.

Remote placement of the A-site 3′end of the tRNA seems to be designed to tolerate variability in PTC binding, as it is required to comply with the ability of the ribosome to accommodate all of the amino acids, to allow for the rotatory motion, and to undergo induced fit of compounds that mimic the real substrate only partially (Schmeing,et al., 2005b). It appears therefore that the tRNA size and shape and the overall ribosome architecture determines the position of the tRNA molecules and the universal base pairs, described above, establish the approximate inclination of the A-site tRNA 3′end, and facilitates P-site meditated catalysis. Accurate A-site tRNA alignment, however, is governed by its remote interactions, and since such placement is the prerequisite for the processivity of protein biosynthesis, it appears that the role played by the remote interactions supersedes all others. This conclusion is supported by the finding that in the absence of these interactions, similar, albeit distinctly different, binding modes are formed, which contrary to substrate orientation

dictated by remote interactions, leads to optimal stereochemistry for the formation of a peptide bond. Hence, binding independent of remote directionality leads to various orientations, each requiring conformational rearrangements to participate in formation of a peptide bond (Moore and Steitz, 2003).

In short, by identifying the linkage between the universal ribosomal symmetry and the substrate binding mode, the integrated ribosomal machinery for peptide bond formation, amino acid polymerization, and translocation within the PTC, was revealed (Agmon et al., 2003; Bashan et al., 2003a). This machinery is consistent with results of biochemical and kinetic studies (Gregory and Dahlberg, 2004; Nierhaus et al., 1980; Sievers et al., 2004; Youngman et al., 2004), proposing that positioning of the reactive groups is the critical factor for the catalysis of intact tRNA substrates, and does not exclude assistance from ribosomal or substrate moieties. Hence, by offering the frame for correct substrate positioning, as well as for catalytic contribution of the P-site tRNA 2'-hydroxyl group, as suggested previously (Dorner et al., 2002; Weinger et al., 2004), the ribosomal architectural-frame governs the positional requirements, and provides the means for substrate mediated chemical catalysis.

2.4. PTC MOBILITY AND ANTIBIOTICS SYNERGISM

The two universally conserved nucleotides A2602 and U2585 that bulge towards the PTC center (Figures 3B and C) and do not obey the symmetry, are extremely flexible. In D50S A2602 is placed beneath A73 of A-site tRNA, within contact distance throughout the course of the rotation. Similarly, U2585, situated under A2602 and closer to the tunnel entrance, is located within a contact distance to bound amino acid throughout the A- to P-site motion. Nucleotide A2602 exhibits a large variety of conformations in different complexes of the large subunit (Agmon et al., 2003; Bashan et al., 2003a). A2602 is involved in several tasks other than peptide bond formation, such as nascent peptide release (Polacek et al., 2003) and anchoring tRNA A- to P-site passage (Agmon et al., 2003, 2005; Bashan et al., 2003a, b; Zarivach et al., 2004).

Sparsomycin, which target A2602 (Bashan et al., 2003a; Hansen et al., 2003; Porse et al., 1999), is a potent universal antibiotics agent, hence less useful as anti-infective drug. Comparisons between sparsomycin binding sites in D50S (Bashan et al., 2003a) and H50S (Hansen et al., 2003) indicated the correlation between antibiotics binding mode and the ribosomal functional-state. By binding to non-occupied large ribosomal subunits, sparsomycin stacks to A2602 and causes striking conformational alterations in the entire PTC, which should influence the positioning of the tRNA in the A-site, thus explaining why sparsomycin was considered to be an A-site inhibitor, although it does not interfere with A-site substrates (Goldberg and Mitsugi, 1966; Monro et al., 1969; Porse et al., 1999). Within D50S, sparsomycin faces the P-site. Hence, it can also enhance nonproductive tRNA-binding (Monro et al., 1969). Conversely, when sparsomycin enters the large subunit simultaneously with a P-site substrate or substrate-analog, it can cause only a modest conformation alteration of A2602, and because the P-site is occupied by the P-site substrate, sparsomycin stacking to A2602 appears to face the A-site (Hansen et al., 2003).

The base of U2585 undergoes a substantial conformational alteration in a complex of D50S with Synercid – a synergetic antibiotic agent, of which one part binds to the PTC and the other blocks the protein exit tunnel (Agmon et al., 2004; Harms et al., 2004). This recently approved injectable drug with excellent synergistic activity, is a member of the streptogramins

antimicrobial drug family in which each drug consists of two synergistic components (SA and SB), capable of cooperative converting weak bacteriostatic effects into lethal bactericidal activity.

In crystals of D50S-Synercid complex, obtained at clinically relevant concentrations, the SA component, dalfopristin, binds to the PTC and induces remarkable conformational alterations; including a flip of 180° of U2585 base hence paralyze its ability to anchor the rotatory motion and to direct the nascent protein into the exit tunnel (Agmon et al., 2004). As the motions of U2585 are of utmost importance to cell vitality, it is likely that the pressure for maintaining the processivity of protein biosynthesis will attempt recovering the correct positioning of U2585, by expelling or relocating dalfopristin, consistent with dalfopristin low antibacterial effect. The SB component of Synercid, quinupristin, is a macrolide that binds to the common macrolide-binding pocket (Auerbach et al., 2004; Schluenzen et al., 2001). Due to its bulkiness, quinupristin is slightly inclined within the tunnel, and consequently does not block it efficiently (Agmon et al., 2004; Harms et al., 2004), thus rationalizing its reduced antibacterial effects compared to erythromycin.

Since within the large ribosomal subunit both Synercid components interact with each other, the nonproductive flipped positioning of U2585 is stabilized, and the way out of dalfopristin is blocked. Hence, the antimicrobial activity of Synercid is greatly enhanced. Thus, the two components of this synergetic drug act in two radically different fashions. Quinupristin, the SB component, takes a passive role in blocking the tunnel, whereas dalfopristin, the SA component, plays a more dynamic role by hindering the motion of a vital nucleotide at the active site, U2585. It is conceivable that such mode of action consumes higher amounts of material, compared to the static tunnel blockage, explaining the peculiar composition of 7:3 dalfopristin/quinupristin in the optimized commercial Synercid, although the crystal structure of the complex D50S-Synercid indicates binding of stoichiometric amounts of both components.

The mild streptogramins reaction on eukaryotes may be linked to the disparity between the 180° flip of U2585 in D50S (Harms et al., 2004) and the mild conformational alterations of U2585 imposed by the SA compounds on eukaryotic or archaeal ribosome, as seen in the complex of H50S with Virginiamycin-M, a streptograminA component (Hansen et al., 2002b). This significant difference in binding modes to eubacterial vs. archaeal ribosomes appears to reflect the structural diversity of PTC conformations (Harms et al., 2001; Yonath, 2002; Yusupov et al., 2001), consistent with the inability of H50S PTC to bind the peptide bond formation blocker clindamycin, as well as the A-site tRNA competitor chloramphenicol (Mankin and Garrett, 1991).

3. On Ribosome Evolution

The entire symmetrical region is highly conserved, consistent with its vital function. Sampling 930 different species from three phylogenetic domains (Cannone et al., 2002) shows that 36% of all of *E. coli* 23S RNA nucleotides, excluding the symmetrical region, are “frequent” (namely, found in > 95% of the sequences), whereas 98% of the symmetrical region nucleotides are categorized as such. The level of conservation increases in the innermost shell of the symmetry related region. Thus, among the 27 nucleotides lying within 10 Å distance from the symmetry axis, 75% are highly conserved, among these seven are absolutely conserved.

The universality of the symmetrical region hints that the ribosomal active site evolved by gene fusion of two separate domains of similar structures, each hosting half of the catalytic activity. Importantly, whereas the ribosomal internal symmetry relates nucleotide orientations and RNA backbone fold (Figure 2), there is no sequence identity between related nucleotides in the A- and the P-regions. The preservation of the three-dimensional structure of the two halves of the ribosomal frame regardless of the sequence demonstrates the rigorous requirements of accurate substrate positioning in stereochemistry supporting peptide bond formation.

Similarly, protein L16, the only ribosomal protein contributing to tRNA positioning (Agmon et al., 2003; Bashan et al., 2003a), displays conserved tertiary structure alongside diverged primary sequence. Consistently, results of recent experiments addressing the functional conservations of the ribosome, show that the translational factor function and subunit–subunit interactions are conserved in two phylogenetically distant species, *E. coli* and T. thermophilus, despite the extreme and highly divergent environments to which these species have adapted (Thompson and Dahlberg, 2004). Similarly, mutations in *T. thermophilus* 16S and 23S rRNAs, within the decoding site and the PTC, produced phenotypes that are largely identical to their mates in mesophilic organisms (Gregory et al., 2005).

The contribution of protein L2 to the ribosomal polymerase activity may also shed some light on ribosome evolution. Protein L2 is the only protein interacting with both the A- and the P-regions (Agmon et al., 2005), and between its two residues involved in these interactions, one (229) was shown to be essential for the elongation of the nascent chain (Cooperman et al., 1995). It appears, therefore, that the main function of L2 is to provide stabilization to the PTC while elongation takes place. Stabilization of the ribosomal frame is mandatory for maintaining accurate substrate positioning, which, in turn, is required for enabling the rotatory motion, but is irrelevant to single peptide bond formation (Yonath, 2003b). This finding is consistent with the assumption that the ancient ribosome was made only from RNA and that the proteins were added later, in order to increase its fidelity and efficiency.

Involvement in maintaining the symmetry region architecture, and consequently in peptidyl transferase activity can also be attributed to protein L36. This small Zn containing protein is situated in the middle of four parallel helixes and seems to stabilize their overall conformation. Two of these helixes are part of the symmetry related region and two are the nonsymmetrical extensions of the PTC main components. Furthermore, at its location, L36 interactions can also connect these helixes with the elongation factors binding sites. Hence, in addition to stabilizing the conformation of the symmetry related region, it may also be involved in transmitting information about factor binding. The possible availability of alternative route for signaling and/or alternative means for conformation preservation, may account for the absence of L36 in some species, such as *H. marismortui.*

4. The Ribosomal Tunnel

4.1. ELONGATION ARREST AND TUNNEL MOBILITY

Nascent proteins emerge out of the ribosome through an exit tunnel, a universal feature of the large ribosomal subunit first seen in the mid-eighties (Milligan and Unwin, 1986; Yonath et al., 1987). This tunnel is adjacent to the PTC and its opening is located at the other end of the subunit (Figure 4). Lined primarily by ribosomal RNA, this tunnel is rather kinked, has a

nonuniform diameter, and contains grooves and cavities (Ban et al., 2000; Harms et al., 2001). Among the few r-proteins reaching its wall, the tips of extended loops of proteins L4 and L22 create an internal constriction.

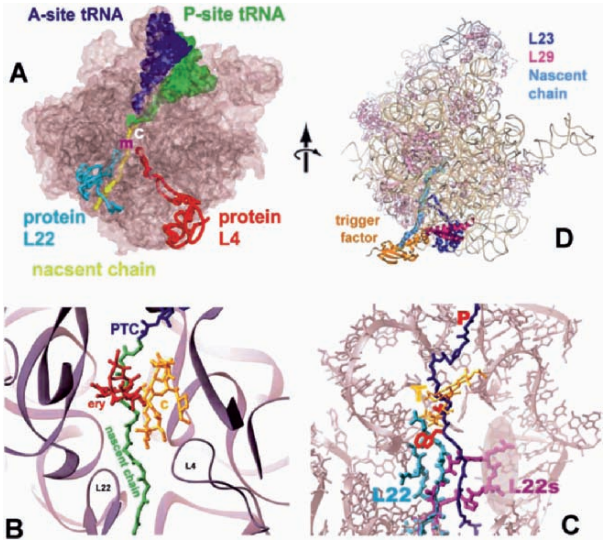

Figure 4. The ribosome tunnel. (**A**) A section through D50S (*in light purple*) with docked A- and P-sites tRNA and modeled polyalanine nascent chain (*yellow*). The approximate positions of the PTC (*P*), the hydrophobic crevice (*C*), and the macrolide pocket (*m*) are marked. The main chains of proteins L4 and L22 are shown in *red* and *cyan*, respectively. (**B**) The hydrophobic crevice (*C*), in relation to the PTC, the macrolide-binding site, represented by erythromycin (ERY), to the tunnel constriction composed of the tips of the elongated loops of proteins L4 and L22, and to the possible pat of the nascent chain (*modeled as polyalanine and shown in green*), Rapamycin binding mode is shown in *gold*. (**C**) A view parallel to the tunnel long axis (*rRNA in olive green*) with a modeled nascent chain (*blue*). The tip of the ribosomal protein L22 beta-hairpin at its native and swung (L22S) conformations, the latter induced by troleandomycin (*T, in gold*) binding, are shown in *cyan* and *magenta*, respectively. The modeled polypeptide chain (*blue*) represents a nascent protein with the sequence motif known to cause SecM (secretion monitor) elongation arrest. This motif is located about 150 residues from the N-terminus and has the sequence XXXWXXXXXXXXXP, where X is any amino acid and P (proline) is the last amino acid to be incorporated into the nascent chain (based on Nakatogawa and Ito, 2002). The positions of two key residues for nascent protein arrest, proline and tryptophane, are highlighted in *red*, to indicate the stunning correlation between its position and that of troleandomycin (*T, in gold*). The specific proline of SecM that is required for the arrest when incorporated into the protein at the PTC is the top amino acid of the modeled nascent chain is designated by P. The shaded area designates the region where mutants bypassing the arrest were depicted (Nakatogawa and Ito, 2002). (**D**) A side view of the structure of trigger factor in complex with D50S (*represented by purple-brown RNA backbone and purple-pink ribosomal proteins*). The bound trigger factor binding domain is shown in *orange*, and a modeled polypeptide chain in *cyan*. Ribosomal proteins L29 and L23 are highlighted in *magenta* and *blue*, respectively. Note the elongated loop of L23, a unique eubacterial feature, which reaches the interior of the tunnel, to a location allowing its interaction with the emerging nascent chain.

Five years ago, when first observed at high resolution in H50S crystal structure, this tunnel was assumed to be a firmly built passive and inert conduit for nascent chains (Ban et al., 2000; Nissen et al., 2000). However, biochemical results, accumulated during the last decade, indicate that the tunnel plays an active role in sequence-specific gating of nascent chains and in responding to cellular signals (Etchells and Hartl, 2004; Gong and Yanofsky, 2002; Johnson, 2005; Nakatogawa and Ito, 2002; Stroud and Walter, 1999; Tenson and Ehrenberg, 2002; Walter and Johnson, 1994; White and von Heijne, 2004; Woolhead et al., 2004). Furthermore, cotranslational folding of nascent polypeptides into secondary structures while still within the ribosomal tunnel has been detected in several cases (e.g. Eisenstein et al., 1994; Hardesty et al., 1995; Woolhead et al., 2004). Such initial folding events within the ribosomal tunnel seem to serve signaling between the cell and the protein-biosynthetic machinery (Johnson, 2005) rather than as segments of the correct fold of the mature protein.

Consistently, the crystal structures of complexes of the large ribosomal subunit from the eubacterium *D. radiodurans*, D50S, revealed a crevice adjacent to the tunnel that can be exploited for initial folding (Figure 4B) (Amit et al., 2005) and indicated that the tunnel has the capability to oscillate between conformations (Figure 4C), and that these alterations could be correlated with nascent protein sequence discrimination and gating (Bashan et al., 2003b; Berisio et al., 2003a), as well as with its trafficking into its chaperone-folding cradle (Baram and Yonath, 2005; Baram et al., 2005). Analysis of these structures also shows that at its entrance, the tunnel diameter may limit the passage of highly folded polypeptides. Furthermore, in specific cases, likely to be connected with nascent chain-tunnel interactions, the tunnel entrance properties accompanied by the incorporation of rigid residues, such as proline, may hamper the progression of protein sequences known to arrest elongation (Gong and Yanofsky, 2002; Nakatogawa and Ito, 2002).

So far most of the tunnel functional roles have been attributed to mobile extended loops of ribosomal proteins that penetrate its walls, which are primarily made of ribosomal RNA. Examples are the tips of extended loops of proteins L22 and L23 that seem to provide communication routes for signaling between the ribosome and the cell, as their other ends are located on the solvent side of the ribosome, in the proximity of the tunnel opening (Baram and Yonath, 2005; Berisio et al., 2003a; Harms et al., 2001). Furthermore, the beta-hairpin tip of L22 can swing across the tunnel around its accurately placed hinge (Figure 4C), and gate the tunnel. This motion appears to provide a general mechanism for elongation arrests triggered by specific cellular conditions, since the interacting nucleotides with the swung L22 hairpin tip are identical to those identified in mutations bypassing tunnel arrest (Agmon et al., 2003; Bashan et al., 2003b; Berisio et al., 2003a). Thus, this elongated ribosomal protein (Harms et al., 2001; Unge et al., 1998) that stretches along the large subunit may not only contribute to the dynamics associated with tunnel arrest, but also participate in signal transmission between the cell and the ribosomal interior.

4.2. INTRA-RIBOSOME CHAPERON ACTIVITY?

The crystal structure is a complex of the large ribosomal subunit from *D. radiodurans*, co-crystallized with rapamycin, a polyketide with no inhibitory activity, revealed that rapamycin binds to a crevice located at the boundaries of the nascent protein exit tunnel, opposite to the macrolide pocket (see below and Figures 4A and B). Being adjacent to the ribosome tunnel, but not obstructing the path of nascent chains at extended conformation, this

crevice may provide the site for local cotranslational folding of nascent chains (Amit et al., 2005). The size of this crevice is suitable for accommodating small secondary structural elements, and therefore may provide nascent chains a site for adopting a particular fold at the early stage of tunnel passage, consistent with a large range of biochemical evidence, obtained mainly for transmembrane proteins, implicating cotranslational folding (Etchells and Hartl, 2004; Johnson, 2005; Stroud and Walter, 1999; Tenson and Ehrenberg, 2002; Walter and Johnson, 1994; White and von Heijne, 2004; Woolhead et al., 2004).

Similar to rapamycin, transmembrane protein segments are highly hydrophobic, and therefore may be accommodated within the crevice. Hence, this crevice may provide the space as well as the hydrophobic patch that might act as an inner-tunnel chaperone, consistent with findings interpreted as nascent chain folding near the PTC, which was proposed to correlate with sequential closing and opening of the translocon at the ER membrane (Woolhead et al., 2004). Hence the detection of the crevice confirms that the tunnel possesses specific binding properties, and suggests that this crevice plays a role in regulating nascent protein progression, thus acting as an intra-ribosome chaperon.

The cotranslational folding may be only transient, until messages are transmitted to other cell components (e.g. the translocon pore) (Etchells and Hartl, 2004; Woolhead et al., 2004). Alternatively, it is conceivable that once small nucleation centers are formed, they may progress through the tunnel by temporary expansions of the tunnel diameter, as observed recently for translation-arrested ribosomes (Gilbert et al., 2004). Cotranslational folding is frequently observed for eukaryotic membrane proteins. These may possess a comparable crevice, as a similar feature could be identified also in the archaeal H50S. However, although existence of a crevice is postulated in ribosomes from all kingdoms of life, this does not imply structural identity, since phylogenetic diversity should play a considerable role in its detailed structure, as found at the macrolide-binding pocket (Auerbach et al., 2004; Baram and Yonath, 2005; Pfister et al., 2004; Yonath, 2005; Yonath and Bashan, 2004). Hence, the binding affinities of this crevice should vary, explaining why rapamycin is not known to strongly inhibit membrane proteins translation.

4.3. THE FIRST ENCOUNTER WITH RIBOSOME ASSOCIATED CHAPERONE

The complex process of folding newly synthesized proteins into their native three-dimensional structure is vital in all kingdoms of life. Although, in principle, protein can fold with no assistance of additional factors, since their sequences entail their unique folds, under cellular conditions nascent polypeptides emerging out of the ribosomal tunnel are prone to aggregation and degradation, and thus require assistance. The cellular strategy to promote correct folding and prevent misfolding involves a large arsenal of molecular chaperones (Bukau et al., 2000; Frydman, 2001; Gottesman and Hendrickson, 2000; Hartl and Hayer-Hartl, 2002; Rospert, 2004; Thirumalai and Lorimer, 2001). These proteins are found in all kingdoms and the existence of ribosome-associated chaperones is a highly conserved principle in eukaryotes and prokaryotes, although the involved components differ between species.

In eubacteria, the folding of cytosol proteins is coordinated by three chaperone systems: the ribosome-associated trigger factor, DnaK, and GroEL. trigger factor (TF), a unique feature of eubacteria, is the first chaperone encountering the emerging nascent chain. This 48 kDa modular protein is composed of three domains, among which the TF N-terminal domain (TFa) that contains a conserved “signature motif”, mediates the association with the ribosome

(Maier et al., 2005). It cooperates with the DnaK system, and their combined depletion causes a massive aggregation of newly synthesized polypeptides as well as cell death above 30°C (Deuerling et al., 1999). Biochemical studies showed that TF binds to the large ribosomal subunit at 1:1 stoichiometry by interacting with ribosomal proteins L23 and L29 (Blaha et al., 2003; Kramer et al., 2002).

Protein L23 exists in ribosomes from all kingdoms of life, but belongs to the small group of ribosomal proteins that display a significant divergence from conservation. Thus, in all species, it is built of an almost identical globular domain. In eubacteria, however, it possesses a unique feature, a sizable elongated loop, which in *D. radiodurans* extends from the vicinity of the tunnel opening all the way into the tunnel interior (Figure 4D) and in (Harms et al., 2001), and can actively interact with the nascent protein passing through it (Baram and Yonath, 2005; Baram et al., 2005), implying a possible dynamic control.

The high resolution crystals structure of D50S in complex with the TFa domain from the same source showed that the "signature motif" and its few amino acids extension (called the "extended signature motif"), interact with the large ribosomal subunit near the tunnel opening (Figure 4D) at a triple junction between ribosomal proteins L23 and L29 and the 23S rRNA (Baram et al., 2005), consistent with a previous suggestion (Kristensen and Gajhede, 2003).

Despite the similarity between the overall structures of the ribosome-bound and the unbound TFa (Ferbitz et al., 2004; Ludlam et al., 2004), significant differences were detected between their conformations and that of the bound TFa, indicating a substantial conformational rearrangement of TFa upon binding to the ribosome. These alterations result in the exposure of a sizable hydrophobic patch facing the interior of the ribosomal exit tunnel, which should increase the tunnel's affinity for hydrophobic segments of the emerging nascent polypeptide. Thus, the trigger factor prevents aggregation of the emerging nascent chains by providing a competing hydrophobic environment (Baram et al., 2005).

In D50S, protein L23 exposes a sticky hydrophobic patch, located in the wall of the ribosomal tunnel and available for interactions with hydrophobic regions of the progressing nascent chain. These interactions may be involved in cotranslational folding of nascent polypeptides into secondary structures while still within the ribosomal tunnel, and such events may trigger signaling to the cell, for recruiting TF and initiating its binding. Thus, the subjection of L23 elongated loop may affect, in turn, its interaction with TF. Similar to the undetected conformational changes in the chimeric complex (Ferbitz et al., 2004), mainly due to the disorder of the corresponding TFa region, the possible involvement of L23 loop in initial folding and/or FT attraction could not be seen in the chimeric complex, since, like in eukaryotes, L23 of H50S lacks the elongate loop that penetrates the tunnel.

It seems, therefore, that protein L23 plays multiple roles in eubacteria. It is essential for the association of TF with the ribosome, and since the tip of its internal loop can undergo allosteric conformational changes thus modulating the shape and the size of the tunnel (Baram and Yonath, 2005; Baram et al., 2005), it may control the pace of the entrance of the nascent chain into its shelter and serve as a channel for cellular communication with the nascent chain while progressing in the tunnel.

5. Antibiotics Targeting the Ribosomal Tunnel

5.1. ANTIBIOTICS SELECTIVITY: THE KEY FOR THERAPEUTIC EFFECTIVENESS

Ribosomes show a high level of universality in sequence and almost complete identity in function, therefore the imperative distinction between pathogens and human, the key for antibiotics usefulness, is achieved by subtle structural difference within the antibiotics binding pockets of the prokaryotic and eukaryotic ribosomes (Auerbach et al., 2004; Yonath and Bashan, 2004). Both *D. radiodurans* and *H. marismortui* are nonpathogenic organisms. Nevertheless, there are major differences between the suitability of their ribosomes to serve as pathogen models. Thus, although *D. radiodurans* is an extremely robust gram-positive eubacterium that can survive in harsh environments, it is best grown under conditions almost identical to those allowing for optimal biological activity of *E. coli* (Harms et al., 2001) and shows striking sequence similarity to it. Moreover, contrary to archaeal and halophilic ribosomes, which possess typical eukaryotic elements at the principal antibiotics targets and are not inhibited by antibiotics at the clinically useful concentrations (Mankin and Garrett, 1991; Sanz et al., 1993), *D. radiodurans* ribosomes are targeted by the common ribosomal antibiotics at clinically relevant concentrations in a fashion similar to most pathogens (Auerbach et al., 2004; Schluenzen et al., 2001). Thus, the availability of structures of antibiotics complexed with ribosomes from both species provides unique tools for investigating the structural basis for antibiotics selectivity.

A striking example is the immense influence of the minute difference between adenine and guanine in position 2058, which was found to dictate the affinity of macrolides binding. Macrolides are natural and semisynthetic compounds, which rank highest in clinical usage. They are characterized by a macrolactone ring to which at least one sugar moiety is attached (Figure 5). The first widely used macrolide drug is erythromycin, a 14-member lactone ring, decorated by a desosamine and cladinose sugars. Ketolides belong to a novel class of the macrolide family, characterized by a keto group at position 3 of the macrolactone ring, a single aminosugar moiety, and an extended hydrophobic arm (Figure 5).

This recently developed drug family was designed to act against several macrolide resistant bacterial strains. Both macrolides and ketolides were shown, crystallographically, to bind to a specific pocket in the eubacterial tunnel, called below the “macrolide-binding-pocket”. Both act by producing a steric blockage of the ribosome exit tunnel, hence hampering the progression of nascent chains (Auerbach et al., 2004; Berisio et al., 2003a, b; Hansen et al., 2002b; Pfister et al., 2004, 2005; Schluenzen et al., 2001, 2003; Tu et al., 2005; Yonath, 2005; Yonath and Bashan, 2004).

This high affinity pocket is composed of nucleotides belonging to the 23S RNA (Figure 5) and is located at the upper end of the tunnel, below the PTC and above the tunnel constriction (Figure 4A). All currently available crystal structures of complexes of 14-membered ring

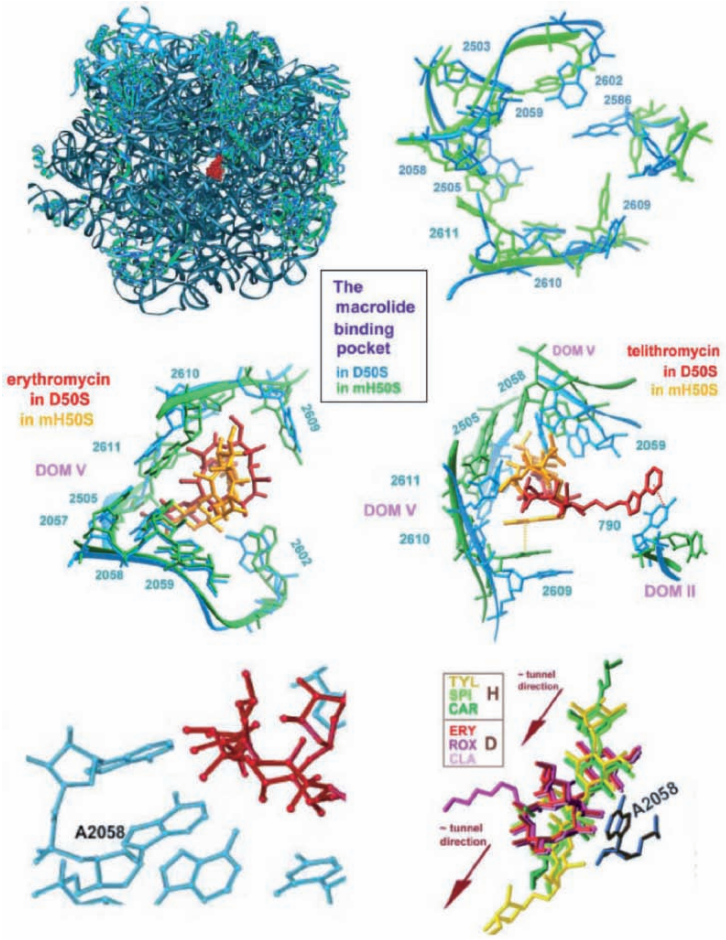

Figure 5. The macrolide-binding pocket. *Top left*: a view into D50S ribosome tunnel, with bound erythromycin (*red*). The ribosomal RNA and ribosomal proteins are shown in *dark* and *light blue*, respectively. *Top right and middle*: the free, erythromycin- and telithromycin-bound pockets, in D50S (*cyan*) and H50S (*green*), highlighting the differences in sequence and orientation (*green letters in parenthesis refer to the type of the nucleotide in H. marismortui if different from that of D. radiodurans*). *In middle right*, the stacking interactions between telithromycin and the binding pocket in both D50S and H50S are shown by *dotted lines*. Note the superiority of tunnel (pocket) blocking in D50S, compared to mH50S. *Bottom left*: Zoom into D50S macrolide pocket (*cyan*), showing the close proximity between 2058 and the bound erythromycin (*red*). *Bottom right*: Superposition of the locations of three 16-membered macrolide tylosin (*TYL*), carbomycin (*CAR*), and spiramycin (SPI) bound to H50S, on the locations of three 14-membered macrolides, erythromycin (ERY), clarithromycin (CLA), and roxithromycin (ROX) bound to D50S, showing that the 16-membered macrolides should not severely hamper nascent protein passage. The location of A2058 and the approximate tunnel direction are also shown. Note the larger distance between the nucleotide at position 2058 and the desosamine sugars of the three 16-member macrolides, compared to the 14-member compounds.

macrolides with large subunits (Berisio et al., 2003a; Schluenzen et al., 2001; Tu et al., 2005) show that the interactions of the desosamine sugar and the lactone ring play a key role in macrolide binding. These contacts involve predominantly the main constituents of the macrolide-binding pocket, namely nucleotides A2058–A2059 of the 23S RNA Domain V (Figures 5A−5D).

The second macrolide sugar, namely the cladinose, interacts directly with the ribosome only in a few cases (Berisio et al., 2003a; Schluenzen et al., 2001). Three closely related 14-membered macrolides, namely erythromycin and its semisynthetic derivatives, clarithromycin and roxithromycin, exhibit exceptional consistency in their binding modes to the macrolide-binding pocket (Figure 5) (Schluenzen et al., 2001). The high binding affinity of these macrolides was found to originate mainly from their interactions with nucleotide 2058. In all eubacteria this nucleotide is an adenine, which provides the means for prominent macrolide interactions. In eukaryotes, as well as in the archaeon *H. marismortui*, it is a guanine.

Consistently, these structures indicated that owing to increased bulkiness, a guanine in position 2058 should impose spatial constrains and hamper macrolide binding, in accord with the resistance mechanisms that are modifying the chemical identity of this nucleotide either by A → G mutation, or by their methylation (Blondeau et al., 2002; Courvalin et al., 1985; Katz and Ashley, 2005; Poehlsgaard and Douthwaite, 2003; Sigmund et al., 1984; Vester and Douthwaite, 2001; Weisblum, 1995). For over three decades it has been known that mutations in proteins L22 and/or L4 can also induce resistance to the 14-membered antibiotics (Davydova et al., 2002; Pereyre et al., 2002; Poehlsgaard and Douthwaite, 2003; Wittmann et al., 1973). Although these proteins are rather close to the macrolide-binding pocket, the structures of the macrolide complexes do not indicate a direct contact with these proteins. Nevertheless, the increase in A2508 size accompanied with the alterations in the tunnel conformation at its constriction, similar or identical to those seen crystallographically (Berisio et al., 2003a) or by electron microscopy (Gabashvili et al., 2001), could be correlated with this antibiotic-resistant mechanism. Thus, at its swung conformation, the tip of protein L22 hairpin loop, reached protein L4.

To circumvent the acute problems associated with macrolide resistance by modification of A2058, several new compounds have been designed. These include macrolide derivatives, in which the core macrolactone ring has been modified, to 15- (e.g. azithromycin) or 16-(tylosin, carbomycin A, spiramycin, and josamycin) membered rings, all exhibiting activity against some MLSB resistance strains (Bryskier et al., 1993; Poulsen et al., 2000). Ketolides present a yet another chemical approach, based on the addition of rather long extensions, such as alkyl-aryl or quinollyallyl, to the core macrolactone ring, expected to provide additional interactions, thus minimizing the contribution of 2058-9 region.

Drug binding to ribosomes with guanine at position 2058 may superficially indicate low level of selectivity, hence 12 ribosomes, nascent proteins, chaperones, and antibiotics should reduce its clinical relevance. This intriguing question triggered a through comparison between antibiotics binding modes to eubacteria, represented by D50S and to eukaryotes, represented by H50S. This comparison revealed a prominent difference in the effectiveness of tunnel blockage (Figure 5), which could be linked to the specific architecture of the two macrolide-macrolide-binding pockets.

Indeed, in H50S there are seven nucleotides that differ from the typical eubacteria, among them three present purine/pyrimidine exchange, and most of the conserved nucleotides have different conformations (Figure 5). Accordingly, the binding modes, and consequently, the therapeutical usefulness of macrolides that bind to H50S, namely the 16-membered ring

compounds (Hansen et al., 2002b) are considerably different from those found in D50S. Thus, in D50S the macrolides occupy most of the tunnel space, whereas in H50S the 16-membered ring macrolides lie almost parallel to the tunnel wall and consume a smaller part of it (Figure 5). These differences are likely to result from the sequence and conformational divergence of the macrolide-binding pocket, in accordance with the low drug affinity to H50S, which forced the usage of immense excess (several orders of magnitude above the clinical levels) of antibiotics for obtaining measurable binding to H50S (Hansen et al., 2002b, 2003), contrary to the usages of clinically relevant drug concentrations in the complexes of D50S (Auerbach et al., 2004; Bashan and Yonath, 2005; Berisio et al., 2003a, b; Harms et al., 2004; Schluenzen et al., 2001, 2003; Yonath, 2005). Hence, the crystallographically observed differences in the antibiotics binding modes demonstrate the interplay between structure and clinical implications and illuminate the distinction between medically meaningful and less relevant binding.

5.2. G → A MUTATION ENABLES MACROLIDES BINDING

Further comparison, supporting the above conclusions, became possible as G2058 in *H. marismortui* 23S rRNA has recently been mutated to an adenosine (Tu et al., 2005). This mutation (called below mH50S) increases macrolide-binding affinity by 10,000-fold, but did not significantly improve the effectiveness of the binding mode, as the magnitude of tunnel blockage in mH50S remains lower than that achieved by the same drug in the eubacterial D50S (Figures 5). Furthermore, based on azithromycin-binding mode to mH50S (Tu et al., 2005), the impressive gain in drug affinity, achieved by the G2058A mutation, is not accompanied by a comparable alteration in its binding mode compared to H50S wild-type, where 2058 is a guanosine. This seemingly surprising finding indicates that although 2058 identity determines whether binding occurs, the conformations and the chemical identities of the other nucleotide in the macrolide pocket govern the antibiotics-binding modes and, subsequently, the drug effectiveness. Interestingly, all mH50S bound macrolides/ketolides share a similar macrolactone conformation, which is almost identical to that suggested by NMR studies to be of the lowest free energy at ribosome-free environments, therefore more likely to occur in vacuum or dilutes solutions. These experiments ignored the ribosome, which by providing a significant interaction network, alters radically the drug environment. Hence, the preservation of conformation of the drug in isolation is inconsistent with the high-binding affinities between ribosomes and macrolides/ketolides.

The case of telithromycin-mH50S complex (Figure 5) supports the separation between binding and effectiveness. Thus, in mH50S telithromycin does not create the prominent interactions of ketolides with domains II (Figure 5), which are consistent with resistance data, and independently identified by footprinting, mutagenesis (e.g. Hansen et al., 1999; Vester and Douthwaite, 2001; Xiong et al., 1999), and crystallographic experiments, using the eubacterium *D. radiodurans* (Berisio et al., 2003a; Schluenzen et al., 2003). Likewise, significant of similarity between the binding modes of telithromycin and erythromycin is inconsistent with the profound differences detected between the susceptibility of A2058G ribosomes to ketolides, as compared with no influence on the susceptibility to macrolides (Pfister et al., 2005).

The rational behind the strange properties of the macrolides/ketolides binding modes to mH50S may be linked to the high salinity (> 2.5 M KCl) essential for *H. marismortui* optimal growth and for maintaining its integrity (Shevack et al., 1985; Yonath, 2002). High salinity is also maintained within H50S crystals, although significantly lower from the optimal value. It is conceivable that in addition to the phylogenetic and conformational variability between archaea and eubacteria, which leads to dissimilarities between antibiotics conformations in D50S vs. H50S-mH50S (Baram and Yonath, 2005; Pfister et al., 2005), the high salinity within the H50S (and mH50S) crystals masks potential ribosomal entities that could have interacted with the drug. The similarity between the conformation of the macrolactone ring of unbound telithromycin, and the resemblance between the binding modes of erythromycin, azithromycin, and telithromycin to H50S and/or mH50S (Tu et al., 2005) support the notion that the high salinity in H50S crystals provides a semi ribosome-free environment to the bound drug, allowing it to maintain its conformation in ribosome-free environment.

To conclude, the G → A mutation of 2058 in *H. marismortui* ribosome was found to be most beneficial for ribosomal-antibiotics research. It confirmed that 2058 is the key player in macrolide binding; it clarified the distinction between mere binding and antibiotics' inhibitory effectiveness; and it provided structural insight into the intriguing question, which is also of utmost importance for drug development: What is the relevance of "minimum free-energy conformation" determined in ribosome-free environment to antibiotics binding and their therapeutic effectiveness? In other words: is there a correlation between the "minimum free-energy conformation" of a drug, determined in ribosome-free environment and its therapeutic effectiveness?

6. Future Expectations

Combating resistance to antibiotics has been a major concern in recent years. However, although pathogens resistant to antibiotics is believed to be the most severe problem in antibiotics usage, in attempts at combating it by novel design and/or by the improvement of existing antibiotics, the selectivity issue must play a key role. Impressive progress has been made by developing chemically improved (e.g. ketolides) as well as synergistic drugs. These open the gates for the introduction of further species-specific anchors, thus increasing selectivity, and for providing alternative interactions, thus reducing the rate of the appearance of resistance. However, the battle is far from its end and additional major effort is necessary.

The conclusions drown from the crystallographic structures of the antibiotics complexes with bacterial ribosome provide indispensable tools for enhancement of the antibiotic efficiency. These structures show that the drugs' chemical properties govern its exact interactions, and that variations in drug properties appear to dominate the exact nature of seemingly identical mechanisms of drug resistance. Hence, the elucidation of common principles, combined with the variability in binding modes, including the discovery of a non-inactivating specific binding to the ribosome, justify expectations for the design of improved antibiotics properties by chemical modifications of existing compounds as well as by the design of novel drugs, based on the structural information.

7. Aknowledgments

Thanks are due to Rita Berisio and to all the members of the ribosome group at the Weizmann Institute for their constant assistance. X-ray diffraction data were collected at ID19/SBC/APS/ANL and ID14/ESRF-EMBL. The US National Institute of Health (GM34360), the Human Frontier Science Program Organization (HFSP: RGP 76/2003), and the Kimmelman Center for Macromolecular Assemblies, provided support. AY holds the Martin and Helen Kimmel Professorial Chair.

References

1. Agmon, I., Auerbach, T., Baram, D., Bartels, H., and Bashan, A., et al. (2003). On peptide bond formation, translocation, nascent protein progression and the regulatory properties of ribosomes. *Eur. J. Biochem.* 270, 2543−2556.
2. Agmon, I., Amit, M., Auerbach, T., Bashan, A., and Baram, D., et al. (2004). Ribosomal crystallography: a flexible nucleotide anchoring tRNA translocation facilitates peptide bond formation, chirality discrimination and antibiotics synergism. *FEBS Lett.* 567, 20−26.
3. Agmon, I., Bashan, A., Zarivach, R., and Yonath, A. (2005). Symmetry at the active site of the ribosome: structure and functional implications. *Biol. Chem.* 386, 833–844.
4. Amit, M., Berisio, R., Baram, D., Harms, J., and Bashan, A., et al. (2005). A crevice adjoining the ribosome tunnel: hints for cotranslational folding. *FEBS Lett.* 579, 3207−3213.
5. Auerbach, T., Bashan, A., Harms, J., Schluenzen, F., and Zarivach, R., et al. (2002). Antibiotics targeting ribosomes: crystallographic studies. *Curr. Drug Targets-Infect Disord.* 2, 169−186.
6. Auerbach, T., Bashan, A., and Yonath, A. (2004). Ribosomal antibiotics: structural basis for resistance, synergism and selectivity. *Trends Biotechnol.* 22, 570−576.
7. Ban, N., Nissen, P., Hansen, J., Moore, P.B., and Steitz, T.A. (2000). The complete atomic structure of the large ribosomal subunit at 2.4 A resolution. *Science* 289, 905−920.
8. Baram, D. and Yonath, A. (2005). From peptide-bond formation to cotranslational folding: dynamic, regulatory and evolutionary aspects. *FEBS Lett.* 579, 948−954.
9. Baram, D., Pyetan, E., Sittner, A., Auerbach-Nevo, T., and Bashan, A., et al. (2005). Structure of trigger factor binding domain in biologically homologous complex with eubacterial ribosome revealed its chaperone action. *Proc. Natl. Acad. Sci. USA* 102, 12017−12022.
10. Barta, A., Dorner, S., and Polacek, N. (2001). Mechanism of ribosomal peptide bond formation. *Science* 291, 203.
11. Bashan, A. and Yonath, A. (2005). Ribosome crystallography: catalysis and evolution of peptide-bond formation, nascent chain elongation and its co-translational folding. *Biochem. Soc. Trans.* 33, 488−492.
12. Bashan, A., Agmon, I., Zarivach, R., Schluenzen, F., and Harms, J., et al. (2003a). Structural basis of the ribosomal machinery for peptide bond formation, translocation, and nascent chain progression. *Mol. Cell* 11, 91−102.
13. Bashan, A., Zarivach, R., Schluenzen, F., Agmon, I., and Harms, J., et al. (2003b). Ribosomal crystallography: peptide bond formation and its inhibition. *Biopolymers* 70, 19−41.
14. Bayfield, M.A., Dahlberg, A.E., Schulmeister, U., Dorner, S., and Barta, A. (2001). A conformational change in the ribosomal peptidyl transferase center upon active/inactive transition. *Proc. Natl. Acad. Sci. USA* 98, 10096−10101.
15. Berisio, R., Schluenzen, F., Harms, J., Bashan, A., and Auerbach, T., et al. (2003a). Structural insight into the role of the ribosomal tunnel in cellular regulation. *Nat. Struct. Biol.* 10, 366−370.

16. Berisio, R., Harms, J., Schluenzen, F., Zarivach, R., and Hansen, H.A., et al. (2003b). Structural insight into the antibiotic action of telithromycin against resistant mutants. *J. Bacteriol.* 185, 4276−4279.
17. Blaha, G., Wilson, D.N., Stoller, G., Fischer, G., and Willumeit, R., et al. (2003). Localization of the trigger factor binding site on the ribosomal 50S subunit. *J. Mol. Biol.* 326, 887−897.
18. Blondeau, J.M., DeCarolis, E., Metzler, K.L., and Hansen, G.T. (2002). The macrolides. *Expert Opin. Investig. Drugs* 11, 189−215.
19. Bocchetta, M., Xiong, L., and Mankin, A.S. (1998). 23S rRNA positions essential for tRNA binding in ribosomal functional sites. *Proc. Natl. Acad. Sci. USA* 95, 3525−3530.
20. Brodersen, D.E., Clemons, W.M., Jr., Carter, A.P., Morgan-Warren, R.J., and Wimberly, B.T., et al. (2000). The structural basis for the action of the antibiotics tetracycline, pactamycin, and hygromycin B on the 30S ribosomal subunit. *Cell* 103, 1143−1154.
21. Bryskier, A., Butzler, J.P., Neu, H.C., and Tulkens, P.M. (1993). Macrolides-Chemistry, Pharmacology, and Clinical Uses. Oxford.
22. Bukau, B., Deuerling, E., Pfund, C., and Craig, E.A. (2000). Getting newly synthesized proteins into shape. *Cell* 101, 119−122.
23. Cannone, J.J., Subramanian, S., Schnare, M.N., Collett, J.R., and D'Souza, L.M., et al. (2002). The Comparative RNA Web (CRW) Site: an online database of comparative sequence and structure information for ribosomal, intron, and other RNAs. *BMC Bioinformatics* 3, 2.
24. Carter, A.P., Clemons, W.M., Brodersen, D.E., Morgan-Warren, R.J., and Wimberly, B.T., et al. (2000). Functional insights from the structure of the 30S ribosomal subunit and its interactions with antibiotics. *Nature* 407, 340−348.
25. Cooperman, B.S., Wooten, T., Romero, D.P., and Traut, R.R. (1995). Histidine 229 in protein L2 is apparently essential for 50S peptidyl transferase activity. *Biochem. Cell. Biol.* 73, 1087−1094.
26. Courvalin, P., Ounissi, H., and Arthur, M. (1985). Multiplicity of macrolide-lincosamide-streptogramin antibiotic resistance determinants. *J. Antimicrob. Chemother.* 16, 91−100.
27. Davydova, N., Streltsov, V., Wilce, M., Liljas, A., and Garber, M. (2002). L22 ribosomal protein and effect of its mutation on ribosome resistance to erythromycin. *J. Mol. Biol.* 322, 635−644.
28. Deuerling, E., Schulze-Specking, A., Tomoyasu, T., Mogk, A., and Bukau, B. (1999). Trigger factor and DnaK cooperate in folding of newly synthesized proteins. *Nature* 400, 693−696.
29. Dorner, S., Polacek, N., Schulmeister, U., Panuschka, C., and Barta, A. (2002). Molecular aspects of the ribosomal peptidyl transferase. *Biochem. Soc. Trans.* 30, 1131−1136.
30. Eisenstein, M., Hardesty, B., Odom, O.W., Kudlicki, W., and Kramer, G., et al. (1994). *Modeling and experimental study of the progression of nascent protein in ribosomes; in Supramolecular Structure and Function*, Pifat, G. (ed.), pp. 213−246, Balaban Press, Rehovot, Israel.
31. Etchells, S.A. and Hartl, F.U. (2004). The dynamic tunnel. *Nat. Struct. Mol. Biol.* 11, 391−392.
32. Ferbitz, L., Maier, T., Patzelt, H., Bukau, B., and Deuerling, E., et al. (2004). Trigger factor in complex with the ribosome forms a molecular cradle for nascent proteins. *Nature* 431, 590−596.
33. Frydman, J., (2001). Folding of newly translated proteins in vivo: the role of molecular chaperones. *Annu. Rev. Biochem.* 70, 603−647.
34. Gabashvili, I.S., Gregory, S.T., Valle, M., Grassucci, R., and Worbs, M., et al. (2001). The polypeptide tunnel system in the ribosome and its gating in erythromycin resistance mutants of L4 and L22. *Mol. Cell* 8, 181−188.
35. Gale, E.F., Cundliffe, E., Reynolds, P.E., Richmond, M.H., and Waring, M.J. (1981). The Molecular Basis of Antibiotic Action, Wiley, London, pp. 419−439.
36. Gaynor, M. and Mankin, A.S. (2003). Macrolide antibiotics: binding site, mechanism of action, resistance. *Curr. Top Med. Chem.* 3, 949−961.
37. Gilbert, R.J., Fucini, P., Connell, S., Fuller, S.D., and Nierhaus, K.H., et al. (2004). Three-dimensional structures of translating ribosomes by cryo-eM. *Mol. Cell* 14, 57−66.
38. Goldberg, I.H. and Mitsugi, K. (1966). Sparsomycin, an inhibitor of aminoacyl transfer to polypeptide. *Biochem. Biophys. Res. Commun.* 23, 453−459.

39. Gong, F. and Yanofsky, C. (2002). Instruction of translating ribosome by nascent peptide. *Science* 297, 1864−1867.
40. Gottesman, M.E. and Hendrickson, W.A. (2000). Protein folding and unfolding by *Escherichia coli* chaperones and chaperonins. *Curr. Opin. Microbiol.* 3, 197−202.
41. Green, R., Samaha, R.R., and Noller, H.F. (1997). Mutations at nucleotides G2251 and U2585 of 23 S rRNA perturb the peptidyl transferase center of the ribosome. *J. Mol. Biol.* 266, 40−50.
42. Gregory, S.T. and Dahlberg, A.E. (2004). Peptide bond formation is all about proximity. *Nat. Struct. Mol. Biol.* 11, 586−587.
43. Gregory, S.T., Carr, J.F., Rodriguez-Correa, D., and Dahlberg, A.E. (2005). Mutational analysis of 16S and 23S rRNA genes of *Thermus thermophilus*. *J. Bacteriol.* 187, 4804−4812.
44. Hansen, L.H., Mauvais, P., and Douthwaite, S. (1999). The macrolide-ketolide antibiotic binding site is formed by structures in domains II and V of 23S ribosomal RNA. *Mol. Microbiol.* 31, 623−631.
45. Hansen, J.L., Schmeing, T.M., Moore, P.B., and Steitz, T.A. (2002a). Structural insights into peptide bond formation. *Proc. Natl. Acad. Sci. USA* 99, 11670−11675.
46. Hansen, J.L., Ippolito, J.A., Ban, N., Nissen, P., and Moore, P.B., et al. (2002b). The structures of four macrolide antibiotics bound to the large ribosomal subunit. *Mol. Cell* 10, 117−128.
47. Hansen, J.L., Moore, P.B., and Steitz, T.A. (2003). Structures of five antibiotics bound at the peptidyl transferase center of the large ribosomal subunit. *J. Mol. Biol.* 330, 1061−1075.
48. Hardesty, B., Kudlicki, W., Odom, O.W., Zhang, T., and McCarthy, D., et al. (1995). Cotranslational folding of nascent proteins on *Escherichia coli* ribosomes. *Biochem. Cell. Biol.* 73, 1199−1207.
49. Harms, J., Schluenzen, F., Zarivach, R., Bashan, A., and Gat, S., et al. (2001). High resolution structure of the large ribosomal subunit from a mesophilic eubacterium. *Cell* 107, 679−688.
50. Harms, J., Schluenzen, F., Fucini, P., Bartels, H., and Yonath, A. (2004). Alterations at the peptidyl transferase centre of the ribosome induced by the synergistic action of the streptogramins dalfopristin and quinupristin. *BMC Biol.* 2, 1−10.
51. Hartl, F.U. and Hayer-Hartl, M. (2002). Molecular chaperones in the cytosol: from nascent chain to folded protein. *Science* 295, 1852−1858.
52. Jencks, W.P. (1969, reissued 1987). Catalysis in Chemistry and Enzymology. Dover Publications, McGraw-Hill, Mineola, NY.
53. Johnson, A.E. (2005). The co-translational folding and interactions of nascent protein chains: a new approach using fluorescence resonance energy transfer. *FEBS Lett.* 579, 916−920.
54. Katz, L. and Ashley, G.W. (2005). Translation and protein synthesis: macrolides. *Chem. Rev.* 105, 499−528.
55. Kim, D.F. and Green, R. (1999). Base-pairing between 23S rRNA and tRNA in the ribosomal A site. *Mol. Cell* 4, 859−864.
56. Knowles, D.J., Foloppe, N., Matassova, N.B., and Murchie, A.I. (2002). The bacterial ribosome, a promising focus for structurebased drug design. *Curr. Opin. Pharmacol.* 2, 501−506.
57. Kramer, G., Rauch, T., Rist, W., Vorderwulbecke, S., and Patzelt, H., et al. (2002). L23 protein functions as a chaperone docking site on the ribosome. *Nature* 419, 171−174.
58. Kristensen, O. and Gajhede, M. (2003). Chaperone binding at the ribosomal exit tunnel. *Structure* 11, 1547−1556.
59. Ludlam, A.V., Moore, B.A., and Xu, Z. (2004). The crystal structure of ribosomal chaperone trigger factor from *Vibrio cholerae*. *Proc. Natl. Acad. Sci. USA* 101, 13436−13441.
60. Maier, T., Ferbitz, L., Deuerling, E., and Ban, N. (2005). A cradle for new proteins: trigger factor at the ribosome. *Curr. Opin. Struct. Biol.* 15, 204−212.
61. Mankin, A.S. and Garrett, R.A. (1991). Chloramphenicol resistance mutations in the single 23S rRNA gene of the archaeon *Halobacterium halobium*. *J. Bacteriol.* 173, 3559−3563.
62. Milligan, R.A. and Unwin, P.N. (1986). Location of exit channel for nascent protein in 80S ribosome. *Nature* 319, 693−695.

63. Monro, R.E., Celma, M.L., and Vazquez, D. (1969). Action of sparsomycin on ribosome-catalysed peptidyl transfer. *Nature* 222, 356−358.
64. Moore, P.B. and Steitz, T.A. (2003). After the ribosome structures: how does peptidyl transferase work? *RNA* 9, 155−159.
65. Nakatogawa, H. and Ito, K. (2002). The ribosomal exit tunnel functions as a discriminating gate. *Cell* 108, 629−636.
66. Nierhaus, K.H., Schulze, H., and Cooperman, B.S. (1980). Molecular mechanisms of the ribosomal peptidyl transferase center. *Biochem. Int*. 1, 185−192.
67. Nissen, P., Hansen, J., Ban, N., Moore, P.B., and Steitz, T.A. (2000). The structural basis of ribosome activity in peptide bond synthesis. *Science* 289, 920−930.
68. Noller, H.F., Hoffarth, V., and Zimniak, L. (1992). Unusual resistance of peptidyl transferase to protein extraction procedures. *Science* 256, 1416−1419.
69. Pereyre, S., Gonzalez, P., De Barbeyrac, B., Darnige, A., and Renaudin, H., et al. (2002). Mutations in 23S rRNA account for intrinsic resistance to macrolides in *Mycoplasma hominis* and *Mycoplasma fermentans* and for acquired resistance to macrolides in *M. hominis*. *Antimicrob Agents Chemother*. 46, 3142−3150.
70. Pfister, P., Jenni, S., Poehlsgaard, J., Thomas, A., and Douthwaite, S., et al. (2004). The structural basis of macrolide-ribosome binding assessed using mutagenesis of 23S rRNA positions 2058 and 2059. *J. Mol. Biol.* 342, 1569−1581.
71. Pfister, P., Corti, N., Hobbie, S., Bruell, C., and Zarivach, R., et al. (2005). 23S rRNA base pair 2057-2611 determines ketolide susceptibility and fitness cost of the macrolide resistance mutation 2058A → G. *Proc. Natl. Acad. Sci. USA* 102, 5180−5185.
72. Pioletti, M., Schluenzen, F., Harms, J., Zarivach, R., and Gluehmann, M., et al. (2001). Crystal structures of complexes of the small ribosomal subunit with tetracycline, edeine and IF3. *EMBO J*. 20, 1829−1839.
73. Poehlsgaard, J. and Douthwaite, S. (2003). Macrolide antibiotic interaction and resistance on the bacterial ribosome. *Curr. Opin. Invest. Drugs* 4, 140−148.
74. Polacek, N., Gomez, M.J., Ito, K., Xiong, L., and Nakamura, Y., et al. (2003). The critical role of the universally conserved A2602 of 23S ribosomal RNA in the release of the nascent peptide during translation termination. *Mol. Cell* 11, 103−112.
75. Porse, B.T., Kirillov, S.V., Awayez, M.J., Ottenheijm, H.C., and Garrett, R.A. (1999). Direct crosslinking of the antitumor antibiotic sparsomycin, and its derivatives, to A2602 in the peptidyl transferase center of 23S-like rRNA within ribosome – tRNA complexes. *Proc. Natl. Acad. Sci. USA* 96, 9003−9008.
76. Poulsen, S.M., Kofoed, C., and Vester, B. (2000). Inhibition of the ribosomal peptidyl transferase reaction by the mycarose moiety of the antibiotics carbomycin, spiramycin and tylosin. *J. Mol. Biol.* 304, 471−481.
77. Rospert, S. (2004). Ribosome function: governing the fate of a nascent polypeptide. *Curr. Biol.* 14, R386−388.
78. Sanz, J.L., Marin, I.R.A., and Urena, D. (1993). Functional analysis of seven ribosomal systems from extreme halophilic archaea. *Can. J. Microbiol.* 35, 311−317.
79. Schluenzen, F., Tocilj, A., Zarivach, R., Harms, J., and Gluehmann, M., et al. (2000). Structure of functionally activated small ribosomal subunit at 3.3 angstroms resolution. *Cell* 102, 615−623.
80. Schluenzen, F., Zarivach, R., Harms, J., Bashan, A., and Tocilj, A., et al. (2001). Structural basis for the interaction of antibiotics with the peptidyl transferase centre in eubacteria. *Nature* 413, 814−821.
81. Schluenzen, F., Harms, J.M., Franceschi, F., Hansen, H.A., and Bartels, H., et al. (2003). Structural basis for the antibiotic activity of ketolides and azalides. *Structure* 11, 329−338.

82. Schluenzen, F., Pyetan, E., Fucini, P., Yonath, A., and Harms, J. (2004). Inhibition of peptide bond formation by pleuromutilins: the structure of the 50S ribosomal subunit from *Deinococcus radiodurans* in complex with tiamulin. *Mol. Microbiol.* 54, 1287−1294.
83. Schmeing, T.M., Seila, A.C., Hansen, J.L., Freeborn, B., and Soukup, J.K., et al. (2002). A pre-translocational intermediate in protein synthesis observed in crystals of enzymatically active 50S subunits. *Nat. Struct. Biol.* 9, 225−230.
84. Schmeing, T.M., Moore, P.B., and Steitz, T.A. (2003). Structures of deacylated tRNA mimics bound to the E site of the large ribosomal subunit. *RNA* 9, 1345−1352.
85. Schmeing, T.M., Huang, K.S., Kitchen D.E., Strobel, S.A., and Steitz T.A. (2005a). Structural insights into the roles of water and the 20 hydroxyl of the P Site tRNA in the peptidyl transferase Reaction. *Mol. Cell* 20, 437–448
86. Schmeing, T.M., Huang, K.S., Strobel, S.A., and Steitz T.A. (2005b). An induced-fit mechanism to promote peptide bond formation and exclude hydrolysis of peptidyl-tRNA, *Nature* 438, 520–525
87. Shevack, A., Gewitz, H.S., Hennemann, B., Yonath, A., and Wittmann, H.G. (1985). Characterization and crystallization of ribosomal particles from *Halobacterium marismortui. FEBS Lett.* 184, 68−71.
88. Sievers, A., Beringer, M., Rodnina, M.V., and Wolfenden, R. (2004). The ribosome as an entropy trap. *Proc. Natl. Acad. Sci. USA* 101, 7897−7901.
89. Sigmund, C.D., Ettayebi, M., and Morgan, E.A. (1984). Antibiotic resistance mutations in 16S and 23S ribosomal RNA genes of *Escherichia coli. Nucleic Acids Res.* 12, 4653−4663.
90. Spahn, C.M. and Prescott, C.D. (1996). Throwing a spanner in the works: antibiotics and the translation apparatus. *J. Mol. Med.* 74, 423−439.
91. Stroud, R.M. and Walter, P. (1999). Signal sequence recognition and protein targeting. *Curr. Opin. Struct. Biol.* 9, 754−759.
92. Schuwirth, B.S., Borovinskaya, M.A., Hau,C.W., Zhang, W., Vila-Sanjurjo, A., Holton, J.M., and Cate, J. (2005). Structures of the bacterial ribosome at 3.5 a resolution. *Science* 310, 827-34.
93. Tan, G.T., DeBlasio, A., and Mankin, A.S. (1996). Mutations in the peptidyl transferase center of 23 S rRNA reveal the site of action of sparsomycin, a universal inhibitor of translation. *J. Mol. Biol.* 261, 222−230.
94. Tenson, T. and Ehrenberg, M. (2002). Regulatory nascent peptides in the ribosomal tunnel. *Cell* 108, 591−594.
95. Thirumalai, D. and Lorimer, G.H. (2001). Chaperonin-mediated protein folding. *Annu. Rev. Biophys. Biomol. Struct.* 30, 245−269.
96. Thompson, J. and Dahlberg, A.E. (2004). Testing the conservation of the translational machinery over evolution in diverse environments: assaying *Thermus thermophilus* ribosomes and initiation factors in a coupled transcription-translation system from *Escherichia coli*. *Nucleic Acids Res.* 32, 5954−5961.
97. Thompson, J., Kim, D. F., O'Connor, M., Lieberman, K. R., Bayfield, M. A., et al. (2001). Analysis of mutations at residues A2451 and G2447 of 23S rRNA in the peptidyltransferase active site of the 50S ribosomal subunit. *Proc. Natl. Acad. Sci. USA* 98, 9002−9007.
98. Tu, D., Blaha, G., Moore, P.B., and Steitz, T.A. (2005). Structures of MLSBK antibiotics bound to mutated large ribosomal subunits provide a structural explanation for resistance. *Cell* 121, 257−270.
99. Unge, J., berg, A., Al-Kharadaghi, S., Nikulin, A., and Nikonov, S., et al. (1998). The crystal structure of ribosomal protein L22 from *Thermus thermophilus*: insights into the mechanism of erythromycin resistance. *Structure* 6, 1577−1586.
100. Vazquez, D. (1979). Inhibitors of protein biosynthesis. *Mol. Biol. Biochem. Biophys.* 30, 1−312.
101. Vester, B. and Douthwaite, S. (2001). Macrolide resistance conferred by base substitutions in 23S rRNA. *Antimicrob Agents Chemother.* 45, 1−12.

102. Walter, P. and Johnson, A.E. (1994). Signal sequence recognition and protein targeting to the endoplasmic reticulum membrane. *Annu. Rev. Cell. Biol.* 10, 87−119.
103. Weinger, J.S., Parnell, K.M., Dorner, S., Green, R., and Strobel, S.A. (2004). Substrate-assisted catalysis of peptide bond formation by the ribosome. *Nat. Struct. Mol. Biol.* 11, 1101−1106.
104. Weisblum, B. (1995). Erythromycin resistance by ribosome modification. *Antimicrob Agents Chemother*. 39, 577−585.
105. White, S.H. and von Heijne, G. (2004). The machinery of membrane protein assembly. *Curr. Opin. Struct. Biol.* 14, 397−404.
106. Wimberly, B.T., Brodersen, D.E., Clemons, W.M., Jr., Morgan-Warren, R.J., and Carter, A.P., et al. (2000). Structure of the 30S ribosomal subunit. *Nature* 407, 327−339.
107. Wittmann, H.G., Stoffler, G., Apirion, D., Rosen, L., and Tanaka, K., et al. (1973). Biochemical and genetic studies on two different types of erythromycin resistant mutants of *Escherichia coli* with altered ribosomal proteins. *Mol. Gen. Genet.* 127, 175−189.
108. Woolhead, C.A., McCormick, P.J., and Johnson, A.E. (2004). Nascent membrane and secretory proteins differ in FRET detected folding far inside the ribosome and in their exposure to ribosomal proteins. *Cell* 116, 725−736.
109. Xiong, L., Shah, S., Mauvais, P., and Mankin, A.S. (1999). A ketolide resistance mutation in domain II of 23S rRNA reveals the proximity of hairpin 35 to the peptidyl transferase centre. *Mol. Microbiol.* 31, 633−639.
110. Yonath, A. (2002). The search and its outcome: high-resolution structures of ribosomal particles from mesophilic, thermophilic, and halophilic bacteria at various functional states. *Annu. Rev. Biophys. Biomol. Struct.* 31, 257−273.
111. Yonath, A. (2003a). Structural insight into functional aspects of ribosomal RNA targeting. *Chem. Biol. Chemistry* 4, 1008−1017.
112. Yonath, A. (2003b). Ribosomal tolerance and peptide bond formation. *Biol. Chem.* 384, 1411−9.
113. Yonath, A. (2005). Antibiotics targeting ribosomes: resistance, selectivity, synergism, and cellular regulation. *Annu. Rev. Biochem.* 74, 649−679.
114. Yonath, A. and Bashan, A. (2004). Ribosomal crystallography: initiation, peptide bond formation, and amino acid polymerization are hampered by antibiotics. *Annu. Rev. Microbiol.* 58, 233−251.
115. Yonath, A., Leonard, K. R., and Wittmann, H. G. (1987). A tunnel in the large ribosomal subunit revealed by three-dimensional image reconstruction. *Science* 236, 813−816.
116. Youngman, E.M., Brunelle, J.L., Kochaniak, A.B., and Green, R. (2004). The active site of the ribosome is composed of two layers of conserved nucleotides with distinct roles in peptide bond formation and peptide release. *Cell* 117, 589−599.
117. Yusupov, M.M., Yusupova, G.Z., Baucom, A., Lieberman, K., and Earnest, T.N., et al. (2001). Crystal structure of the ribosome at 5.5 A resolution. *Science* 292, 883−896.
118. Zarivach, R., Bashan, A., Berisio, R., Harms, J., and Auerbach, T., et al. (2004). Functional aspects of ribosomal architecture: symmetry, chirality and regulation. *J. Phys. Org. Chem.* 17, 901−912.